THE ASTROPHYSICAL JOURNAL, 347:373–391, 1989 December 1

WOLF-RAYET STARS IN THE MAGELLANIC CLOUDS. VII. SPECTROSCOPIC BINARY SEARCH AMONG THE WNL STARS AND THE WN6/7–WN8/9 DICHOTOMY[1]

ANTHONY F. J. MOFFAT[2,3]
Département de physique, Université de Montréal
Received 1989 February 7; accepted 1989 June 1

ABSTRACT

Late-type Wolf-Rayet (W-R) stars of the nitrogen sequence (WNL) can be sensibly divided into two groups: (1) WN6, WN7 and (2) the cooler WN8, WN9 stars. The latter generally have narrower emission lines and relatively strong He I P Cygni profiles. In either the LMC or the Galaxy, $\sim\frac{1}{4}$ of all W-R stars are WNL; of these, $\sim\frac{1}{4}$ are WN8,9. All massive stars that later become W-R stars, probably start as WNL.

None of the nine monitored WN8,9 stars in the LMC and the Galaxy shows W-R + O binary-related radial velocity variations. This is in stark contrast with the 58% W-R + O binary frequency among the 26 monitored WN6,7 stars. This fraction is the same in each galaxy. Orbital masses of WN6,7 stars lie in the range $\sim$30–60 $M_\odot$, with binary mass ratios $M(\mathrm{WN6,7})/M(\mathrm{O}) \gtrsim 1$.

WN8,9 stars are much more dispersed in space than WN6,7 stars, which tend to be found in clusters. While WN8,9 stars have slightly fainter mean visual absolute magnitudes ($M_v = -5.6 \pm 0.3$) than WN6,7 stars ($M_v = -6.1 \pm 0.2$), possibly a result of crowding and duplicity of the WN6,7 sample, both groups show similar, relatively large dispersion in absolute magnitude [$\sigma(M_v) \sim 0.8$–0.9 mag]. However, WN8,9 stars are considerably more variable than WN6,7 (or any other W-R) stars. The basic reason for the often strong differences between these two groups is unknown.

Subject headings: galaxies: Magellanic Clouds — stars: binaries — stars: Wolf-Rayet

I. INTRODUCTION

In the Galaxy, it is generally thought that all stars with initial mass above 30–40 $M_\odot$ eventually evolve through the Wolf-Rayet (W-R) phase. Although the winds of W-R stars have high speeds, similar to those of their O-type progenitors, they are generally at least an order of magnitude denser than O-star winds. W-R winds show the products of various degrees of nuclear burning, depending on the sequence (WN, WC, WO) and probably also on the subtype within each sequence (e.g., C/He increases from WC7 to WC4 according to Smith and Hummer [1988]; but cf. Torres [1988] and de Freitas Pacheco and Machado [1988]).

The first W-R phase encountered by massive stars is likely the WNL phase, characterized by relatively narrow emission lines, much like those seen in the Of phase, which is intermediate between nonemission O stars and the more developed WNE/WC stars with much stronger, broader lines (Conti 1976). That all stars above 30–40 $M_\odot$ probably start their W-R evolution as WNL stars is supported by the fact that, unlike WNE, WC, and WO stars, WNL stars are found at all galactocentric distances in the disk (van der Hucht *et al.* 1988). WNL stars are also the most luminous and massive of the W-R stars, as expected if they resemble most their O-type progenitors before the high W-R mass loss reduces their masses and luminosities.

Subsequent evolution after WNL to WNE, WCL, and WCE/WO stars before they explode as supernovae is controversial. The simplest scenario follows the intuitive idea of a wind-induced peeling-off process, whereby hotter layers of more and more nuclear processed material are exposed. Moffat (1981, 1982) proposed that (1) WNL stars evolve into WNE stars mainly in low-metallicity (Z) environments such as the outer Galaxy and the Magellanic Clouds (MC) and (2) WNL stars evolve more quickly to WCL for high Z such as in the inner Galaxy. Either of these paths could be followed by WCE → WO. How far along this evolutionary sequence a star proceeds may depend on its initial mass. This scenario is supported in particular by (*a*) the overall space distribution in the Galaxy and the MCs (van der Hucht *et al.* 1988; Breysacher 1986; Moffat 1988), (*b*) continuity of mass ratios (Moffat 1981, 1982), which tend to decrease from cool to hot subtypes in each W-R sequence, (*c*) continuity of luminosity (Lundström and Stenholm 1984), which also tends to decrease in the same way as mass ratio with subtype, and (*d*) continuity of the shapes of spectral emission lines.

An important question for W-R stars is the binary frequency. Although it is no longer believed to be 100%, the binary frequency may be correlated with ambient metallicity: when Z is low, wind-induced mass loss is less effective (Abbott 1982; but cf. Garmany and Fitzpatrick 1988), while mass transfer in massive binaries is unaffected. This could explain why there are relatively more binaries in low-Z samples (Hidayat, Admiranto, and van der Hucht 1984). The present work is intended to concentrate on the binary frequency among WNL stars in the LMC, based on spectroscopic radial velocity (RV) monitoring. Comparison with the Galaxy will be made, masses derived and other properties of WNL stars discussed.

Papers I–IV in this series have dealt with spectroscopic and RV studies of individual W-R stars in the MCs. Paper V summarizes the work on all eight SMC stars, while paper VI deals with the brighter WC binaries in both clouds (Moffat, Niemela,

[1] Based partly on observations collected at the European Southern Observatory (ESO), Chile.

[2] Visiting Astronomer, Cerro Tololo Inter-American Observatory (CTIO), National Optical Astronomical Observatories, operated by the Association of the Universities for Research in Astronomy, Inc., under contract with the National Science Foundation.

[3] Alexander von Humboldt Research Fellow, Universität Bonn, 1982–1983.

and Marraco 1989; this paper also gives the references to papers I–V).

II. THE WNL POPULATION

The LMC contains some 100 W-R stars (Breysacher 1981, 1986), of which 24 objects (see Table 1), some multiple W-R stars, are WNL. In the Galaxy, interstellar extinction in the disk has prevented us from uncovering more than the present ~160 known W-R stars (van der Hucht *et al.* 1988) (although further searches to fainter magnitudes are underway: see Shara *et al.* 1989), of which 53 (see Table 2) are WNL. Relative numbers in the Galaxy and the MCs are compared in Table 3. The fraction of WNL stars is seen not to vary significantly from one galaxy to another. The slightly higher fraction for the Galaxy should be regarded as an upper limit, since we are dealing with a magnitude rather than a volume-limited sample, in which the intrinsically brighter WNL stars are seen out to larger distances. It is probably safe to say that roughly $\frac{1}{4}$ of all W-R stars are of type WNL, regardless of Z.

It is instructive to subdivide WNL stars into two groups: (1) the WN8 and WN9 stars, which generally have slower winds and relatively strong P Cygni profiles for some lines even in their visible spectra, and (2) the WN6 and WN7 stars, which have faster winds and weak, if at all, P Cygni profiles in the visible, often along with blueshifted O-star–like photospheric absorption lines. Note that there is much less difference (sometimes even confusion) in classifying WN8 versus WN9 or WN6 versus WN7 stars, compared to WN8,9 versus WN6,7.

In Table 3, we see that about $\frac{1}{4}$ of all WNL stars are of type WN8,9, independent of the environment. The Galactic data for WN8,9 refer to a slightly smaller volume than that for WN6,7 which are somewhat brighter intrinsically on the average (cf. § V). Allowing for this will increase the Galactic fraction of WN8,9 stars, more in line with the LMC, in which the sample should be fairly complete. However, the WN8,9 stars tend to be much more dispersed in their spatial distribution than WN6,7 stars, which are often found in tight groups and very young clusters. This is especially evident in the LMC (Fig. 1): the giant H II region and starburst core of 30 Dor (diameter

TABLE 1

WN6–9 STARS IN THE LMC

Br[a]	HD/Other	Adopted Spectral Type	v	M_v	RV Orbit	P (d)	K(WNL) (km s^{-1})	$f(m)$ ($M_\odot$)
13......	33133	WN8	12.7	−6.1	Const.			
18......	E269227/R84	WN9	12.1	−6.7	Const.			
24......	FD 23	WN7	13.4	−5.4				
26......	36063	WN7	12.7	−6.1	SB1	1.9075	231	2.4
36......	FD 30	WN8	13.5	−5.5				
44a.....	...	WN8-9	14.3	−4.5				
47......	FD 42	WN8	14.9:	−4.1:				
57......	FD 53	WN6	14.0	−5.1				
64......	FD 56	WN9	13.5	−5.7				
65......	E269828	WN7*	13.9:*	−5.3:	SB1	3.0032	238	4.2
71......	E269883	WN7	13.8	−5.4				
72......	E269891/R130	WN6 + B1 Ia*	11.5	−7.7	SB1(W-R)	4.3092	204	3.8
73......	AB 10	WN7*	14.0*	−5.1	Const.			
75......	FD 63/R134	WN7*	12.6	−6.6	Const.			
79......	AB 12	WN6	13.7	−5.5				
80......	FD 64/R135	WN7	13.2	−6.0				
81......	AB 11	WN8	13.8	−5.4				
82......	38268/R136a	WN6 + O5*	>11.4:*	($n \approx$ 4-5W-R)	SB1	4.377	37	0.02 (observed) (1.5, 2.9 for n = 4,5 W-R)
—......	R136c	WN6	12.4:	−6.8:				
87......	FD 68/R140a2	WN6	>12.3:*	>−6.9:	SB1	2.7596	70	0.10 (observed) (0.8 for n = 2 W-R)
—......	R140b	WN6	12.5:	−6.7:				
89......	38282/R144	WN7	11.2	−8.0	Const.			
90......	E269928/R145	WN7	12.2	−7.0	SB1	25.17:	82	1.4:
92......	38344/R147	WN6	13.1	−6.1	Const.			
91......	AB 13	WN9	12.7*	−6.4	Const.			
				Nonpure W-R with RV				
86......	FD 67/R139	WNL/Of	11.9	−7.3	SB1	52.7:	67	1.6:

NOTES.—1. The table includes all stars of type WN6–WN10 from Breysacher (1981, 1986). Exluded are WN5,6 stars, WNL/Of stars (Br 76, 77, 78, 86; cf. Moffat *et al.* 1987, although Br 86 was originally included in the original RV program and is retained here).

2. Spectral types adopted are an average of the types given by Breysacher (1981, 86); Conti, Leep, and Perry (1983); and the present spectra. Exceptions (*) are: Br 65, in a very crowded group, has been resolved with the present spectra; Br 72 and Br 82 have been studied in detail by Moffat and Seggewiss (1986) and Moffat, Seggewiss, and Shara (1985), respectively; Br 73 is extremely crowded—for it and Br 75 the present spectra clearly show N III stronger than N IV. Note that some stars given as WNL by Breysacher (1981) are now clearly not so (e.g., the crowded star Br 83 classified WN6 is now known to be WC5; see Moffat *et al.* 1987).

3. All stars appear visually single in $\lesssim 1''$ seeing except Br 65, Br 73, Br 82, Br 87, and Br 91 (denoted by *). Magnitudes have been adopted from Breysacher (1981) except for these five systems, for which fainter, revised values are given based on visual estimates or recent revisions as follows: Br 65 is identified by Lortet and Testor (1988) who give v = 13.9. Br 73 has been isolated at v = 14.0 by Testor, Llebaria, and Debray (1988).

4. The RV amplitude K is based on the narrow, symmetric line N IV 4058.

[a] Stars Br 71–92 are in the 30 Dor core, stars Br 13–47 are well outside the core, and stars Br 57–65 and Br 91 are at the fringes of the core.

TABLE 2

GALACTIC WN6–9 STARS

WR	HD/Other	Adopted Spectral Type	v	$b-v$	RV Orbit	e	P (d)	K(WNL) (km s^{-1})	$f(m)$ ($M_\odot$)	Reference
8	62910	WN6 + WN4	10.56	+0.43	SB2?	0.4:	85.37:	30:	0.2	1
12	CD −45°4482	WN7	11.06	+0.48	SB1	0	23.9	130	5.5	1
16	86161	WN8	8.43	+0.25	SB1l?	0	10.73	6	0.00024	2
22	92740	WN7 + a	6.44	+0.03	SB1	0.6	80.35	70	1.5	3, 4
24	93131	WN7 + a	6.49	−0.06	Const.					3, 4
25	93162	WN7 + a	8.17	+0.29	Const.					5, 4
28	MS 2	WN7	12.98	+0.72						
29	MS 3	WN7	12.65	+0.64						
35	MS 6	WN6	13.83	+0.75						
40	96548	WN8	7.85	+0.11	SB1l?	0	4.762	9	0.0004	6
43	97950	WN6 + O5	(10.02	+1.06)	Contains SB(1)	0	3.7720	72	(0.15)	7
47	E311884	WN6 + O5V	11.09	+0.72	SB2	0	6.34	277	14	8
55	117688	WN7	10.87	+0.40						
62	NS 2	WN6	14.22	+1.60						
63	LSS 3289	WN6	12.81	+1.28						
66	134877	WN8	11.71	+0.73						
67	LSS 3329	WN6	12.21	+0.74						
71	143414	WN6	10.22	+0.06	SB1l?	0	7.690	21	0.007	9
74	BP 1	WN7	14.01	+1.52						
75	147419	WN6	11.42	+0.63						
78	151932	WN7	6.61	+0.21	Const.					10
82	LS 11	WN8	12.42	+0.81						
83	He3-1344	WN6	12.79	+0.65						
84	The 3	WN6	13.55	+1.18						
85	LSS 3982	WN6	10.60	+0.56						
87	LSS 4064	WN7	12.59	+1.34						
89	LSS 4065	WN7	11.53	+1.22						
91	StSa 1	WN7	(15.0)							
94	158860	WN6	12.22	+0.74						
98	E318016	WN7 + WC7	12.51	+1.08						
100	E318139	WN6	13.44	+1.17						
105	NS 4	WN8	12.92	+1.84:						
107	DA 1	WN7–8	14.10	+1.32:						
108	E313846	WN9	10.14	+0.70	Const.					11
110	165688	WN6	10.30	+0.25	Const.					12
115	IC 14-19	WN6	12.32	+1.10						
120	Vy 1-3	WN7	12.30	+1.02						
123	177230	WN8	11.26	+0.43	SB1l?	0	1.7616	22	0.0020	11
124	209 BAC	WN8	11.58	+0.81	SB1l?	0	2.3583	13	0.0005	13
130	LS 16	WN8	12.60	+1.18						
131	IC 14-52	WN7 + a	12.36	+0.73						
134	191765	WN6	8.23	+0.20	SB1l?	0	7.44	20	0.006	14
136	192163	WN6	7.65	+0.23	SB1l?	0	4.5	8	0.00024	15
					SB1l?	0	2.3238	16	0.0010	
138	193077	WN6 + a	8.10	+0.22	+					16
					SB2?	0:	1763:	31	5.5	
141	193928	WN6	10.14	+0.71	SB1	0	21.64	130	4.9	17
145	AS 422	WN7 + WC4	12.55	+1.63	SB1	0	22:	150	7.7:	18
147	NS 6	WN7	14.89	+2.15						
148	197406	WN7	10.46	+0.36	SB1	0.1	4.317364	86	0.28	19
149	ST 4	WN6	14.70	+1.20						
153	211853	WN6 + O	9.08	+0.27	SB(2)	0	6.6884	247	10.5	20
155	214419	WN7	8.75	+0.28	SB1	0	1.641245	310	5.1	21
156	AC +60°38562	WN8	11.09	+0.83	Const.					11
158	AS 513	WN7	11.46	+0.75	Const.					11

NOTES.—Source of stars and spectral types: van der Hucht *et al.* (1988), with some modifications for some stars as listed below.

WR 8: K(WC4) $\simeq$ 100 km s^{-1} in antiphase with the WN6 component. Thus M(WC4)/M(WN6) $\simeq$ 0.3, in agreement with the overall trend of mass ratios (Moffat 1981, 1982). However, the binary nature of this star has not been unequivocally established.

WR 43: Core of the dense cluster NGC 3603. Taking three similar W-R stars in the slit yields a corrected value $K' \approx 3$ K = 216 km s^{-1} and $f'(m) = 4\ M_\odot$.

WR 47: One of the rare double-line binaries among WNL stars; also the most massive known W-R star. The mass ratio is M(WN6)/M(O5 V) = 0.84. The orbital inclination from polarimetric and photometric monitoring is $i = 70°$ (Moffat *et al.* 1989).

WR 138: This may be a triple system. The longer period involving the two spectroscopically visible stars yields a mass ratio M(WN6)/M(O) $\simeq$ 1.4.

WR 148: This star has the smallest mass function among all SB1, SB2 WNL systems, neglecting the WNL + neutron star (i.e. SB1l) candidates. The orbital inclination from polarization monitoring is $i = 67°$.

WR 153: This is a quadruple system; K(O) = 56 km s^{-1} (paired with the W-R star) is blended with the second O + O pair. Orbital inclination $i = 78°$ from polarimetry (St.-Louis *et al.* 1988).

WR 155: Analysis of the light curve gives M(WN7)/M(O) $\simeq$ 1.33. The orbital inclination from polarization is $i = 78°$ (Drissen *et al.* 1986*b*).

REFERENCES.—(1) Niemela 1982; (2) Moffat and Niemela 1982; (3) Moffat and Seggewiss 1978; (4) Conti, Niemela and Walborn 1979; (5) Moffat 1978; (6) Moffat and Isserstedt 1980; (7) Moffat and Niemela 1984; (8) Niemela, Conti, and Massey 1980; (9) Isserstedt, Moffat, and Niemela 1983; (10) Seggewiss and Moffat 1979; (11) Lamontagne, Moffat, and Seggewiss 1983; (12) Lamontagne 1983; (13) Moffat, Lamontagne, and Seggewiss 1982; (14) Antokhin, Aslanov, and Cherepashchuk 1982; (15) Koenigsberger, Firmani, and Bisiacchi 1980; (16) Lamontagne *et al.* 1982; (17) Bracher 1966; (18) Pesch, Hiltner, and Brandt 1960; (19) Drissen *et al.* 1986*a*; (20) Massey 1981; (21) Leung, Moffat, and Seggewiss 1983.

TABLE 3

WNL POPULATIONS

Quantity	The Galaxy	LMC	SMC
Total no. W-R	160 (known)	100	8
No. WNL (% of W-R)	53[a] (33%)	28[b] (28%)	2[c] (25%)
No. WN6/7 (% of WNL)	42.5[d] (80%)	20 (71%)	2 (100%)
No. WN8/9 (% of WNL)	10.5 (20%)	8 (29%)	0 (0%)

[a] Upper limit for a magnitude-limited sample.

[b] Taking four WNL stars in R136a, all of type WN6/7.

[c] One of these may be of intermediate type, WNL/Of (Conti, Massey, and Garmany [1989] find these two stars to be WN4.5).

[d] Noninteger arises from one dual WN7–8 subtype assignment.

$\sim 10'$) contains only one WN8,9 star compared to ~ 16 WN6,7 stars, in contrast with the ratio 8:3 for WN8,9 versus WN6,7 in the rest of the LMC.

Already from Galactic data, we note (Table 2) that those WNL stars for which RV variability has been investigated, the binary frequency (W-R + O, SB2 or SB1) is normal ($\sim 60\%$) for WN6,7 stars, while it is low (0/6) for WN8,9 stars. These statistics will be verified by checking for massive binaries among the present sample of WNL stars in the LMC.

III. OBSERVATIONS

Photographic image-tube spectra ($\lambda\lambda 3700$–5000, resolution, ~ 1.5 Å) were obtained during four observing runs from 1978 to 1982 at the CTIO 1 m telescope. RVs were derived through bisection of a parabola fitted to the line cores in photographic density (without rectification, since the lines are generally narrow). More details of the procedure are given in the previous papers of this series.

These data were supplemented in the case of the star Br 26 by IDS spectra obtained at the ESO 1.5 m telescope (see Moffat, Seggewiss, and Shara 1985, hereafter MSS, for more details).

Among the 25 WNL objects listed in Table 1, a total of 13 have now been monitored for RV variability. These are generally among the brighter WNL stars in the LMC. Of these 13, three have been published separately elsewhere (Br 72 = R130: Moffat and Seggewiss 1986; Br 82 = R136a: Moffat and Seggewiss 1983, MSS; Br 87 = R140a: Moffat *et al.* 1987). We also observed the bright WNL/Of star Br 86 = R139 in 30 Dor, since it was originally thought to be a genuine W-R star (Breysacher 1981).

Some of the stars in Table 1 turned out to be very close visual systems (WN6,7 only!). Their magnitudes (Breysacher 1986) have been corrected as much as possible in the table (as noted there), based on a combination of visual inspection at the telescope in good seeing, direct images, and relative exposure times. Spectral subtypes (Breysacher 1986) have also been modifed where appropriate, based on the present spectra.

Mean photographic spectra are shown in Figure 2 for the 11 LMC stars discussed in this paper; the spectral subtypes are well behaved according to the classification criteria of Smith (1968), modified by van der Hucht *et al.* (1981). Mean spectra of some stars based mainly on IDS data are also shown in previous papers (Br 72 = R130, Br 75 = R134, Br 82 = R136a, R136c, R140b, Br 90 = R145 for $\lambda\lambda 4400$–4800 in MSS; Br 87 = R140a, R140b for $\lambda\lambda 3700$–5000 in Moffat *et al.* 1987; Br 26, Br 72 = R130 for $\lambda\lambda 3700$–5000 in Moffat and Seggewiss 1986).

IV. RESULTS FOR INDIVIDUAL STARS

These will be presented in order of right ascension.

a) Br 13, WN8

A detailed list of RVs is given in Table 4 for the 14 strongest lines, including three He I P Cygni absorption features. No nebular emission lines are seen. The strongest (symmetric) line, He II 4686, shows relatively small scatter, σ (RV) ~ 9 km s^{-1}, with only a small change in the mean over the year interval

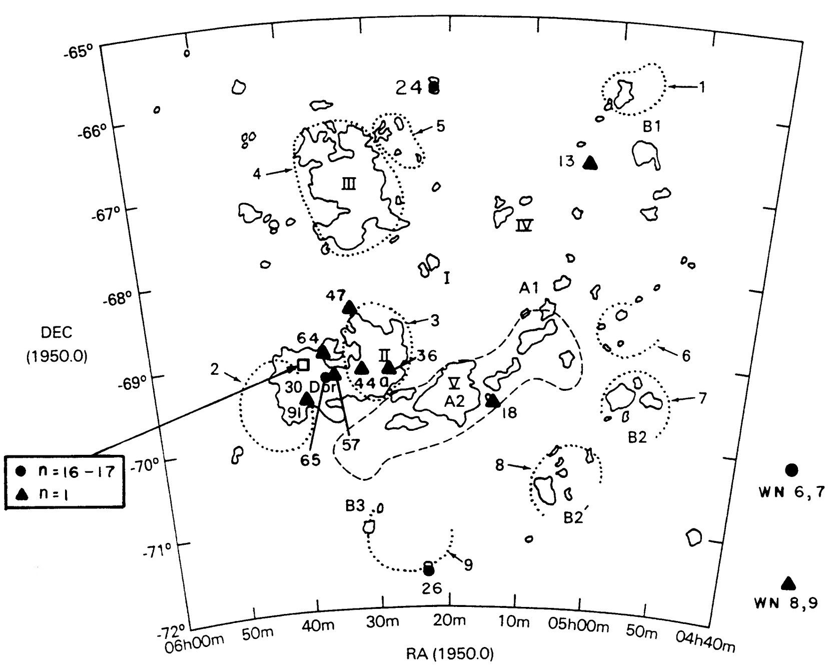

FIG. 1.—Distribution of WN6,7 and WN8,9 stars over the face of the LMC. The map is from Smith, Cornett, and Hill (1987). Numbers are Br identifications as in Table 1.

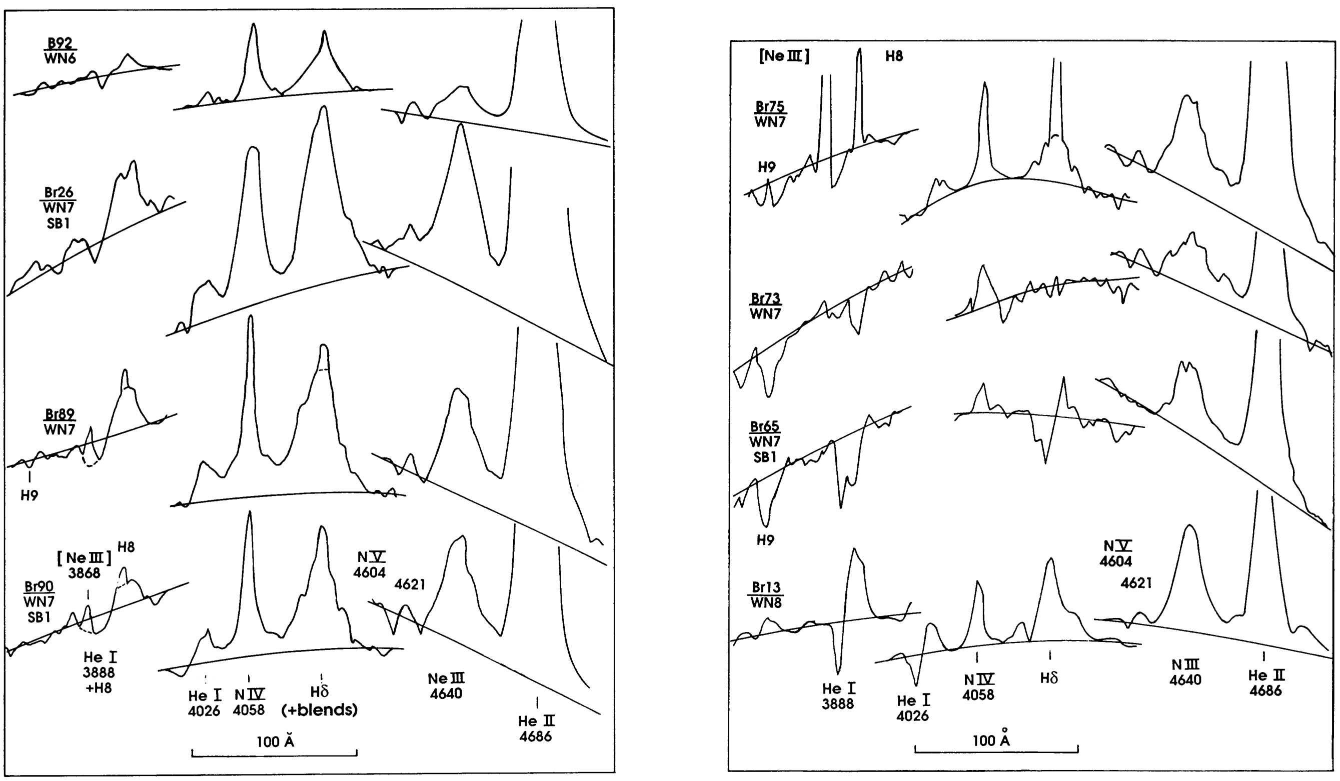

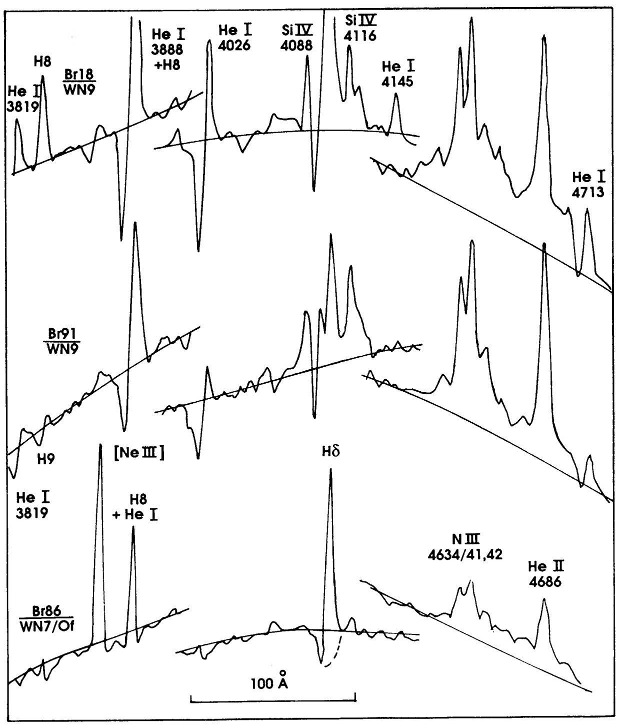

FIG. 2.—Mean photographic density (~log intensity) for the key regions of the spectra of the 11 LMC stars studied intensively here. All are at the same scale except Br 92 and Br 13 which are compressed by a factor 2.6 in ordinate.

between the two data sets (-10 ± 4 km s^{-1}). Other emission lines show different sign changes between the two epochs. A formal sine-wave period search yielded the most significant period $P = 2^{d}.722$ and RV amplitude $K = 9 \pm 2$ km s^{-1} for He II 4686. However, the N IV 4058 line shows only antiphased RV variations with this period, excluding any reasonable likelihood of a WN8 + c (low-mass, compact companion) system. Thus, it is concluded that Br 13 does not vary significantly in RV on any time scale from a day to a year and can be labeled as a probable single star.

b) *Br 18, WN9*

This star shows even narrower W-R lines than Br 13 (and no nebular emission lines), with σ(RV) $\simeq 5$ km s^{-1} for He II 4686, the strongest line. Lacking variations on time scales from a day to a year (see Table 5), this star is thus very likely single.

c) *Br 26, WN7*

A cursory inspection of the RVs in Tables 6 and 7 immediately reveals large variations. A periodic search among the strongest emission lines (there are no photospheric absorption lines visible) yields $P = 1^{d}.9075 \pm 0^{d}.0002$, making Br 26 the shortest known W-R binary system in the LMC (although the WC4 + O6 system Br 32 is close behind, with $P = 1^{d}.91674$: see paper VI) and the shortest of all W-R binaries after the Galactic WN7 system CQ Cep ($P = 1^{d}.64$). Results of orbital fits are given in Table 8 and shown for the best lines in Figures 3*a* and 3*b*. As for CQ Cep, they show greatest RV amplitude for weaker lines of highest excitation, i.e., lines formed closest to the W-R star, where perturbations by the O companion are likely to be least. In particular, He II 4686 has about half the amplitude of the N IV and the Pickering He II lines. He II 4686 and N III 4638 are also significantly phase-shifted in RV.

TABLE 4

Radial Velocities of Br 13 (WN8)

JD-2,440,000	He Ia 3888.646	He Ie 3888.646	He Ia 4026.189	He Ie 4026.189	N IVe 4057.759	Hδe 4101.737	He IIe 4199.830	Hγe 4340.468	He Ia 4471.507	He Ie 4471.507	He IIe 4541.590	N IIIe 4638	He IIe 4685.682	Hβe 4861.332
4585.672	−453	417	−373	405	203	306	373	377	−412	503	332	299	331	300
4586.669	−457	375	−342	362	195	339	361	328	−364	386	360	314	341	325
4587.781	−454	378	−348	436	254	368	390	345	−359	384	366	299	322	330
4588.805	−470	403	−406	403	201	342	404	322	−393	381	391	300	331	358
4589.747	−480	392	−364	437	220	355	323	337	−402	371	352	295	329	311
4595.700	−440	415	−263	383	245	380	421	321	−357	367	398	272	328	342
4596.759	−467	404	−323	372	201	357	349	388	−352	331	346	284	334	348
4597.663	−477	358	−301	403	205	330	361	309	−375	441	391	305	343	319
4599.675	−461	390	−334	461	250	346	376	325	−360	345	358	311	342	331
4974.682	−442	423	−343	451	228	356	310	347	−362	394	414	281	320	324
4975.790	−430	438	−334	393	196	359	459	358	−381	372	386	313	332	327
4976.679	−457	435	−381	444	202	360	372	356	−390	463	414	255	323	305
4978.699	−479	374	−371	424	191	351	337	357	−427	463	344	275	325	313
4979.628	−506	374	−428	412	237	371	340	322	−399	362	365	255	309	309
4980.692	−512	406	−341	436	226	363	332	399	−384	351	358	273	325	313
4981.668	−499	382	−281	500	226	366	380	334	−329	428	422	296	333	326
4982.655	−468	385	−338	405	221	388	324	354	−337	375	369	293	315	336
Mean	−467	397	−345	419	218	355	365	346	−375	395	374	289	328	325
σ	23	23	41	35	20	19	39	25	26	48	27	19	9	16
1980 mean	−462	392	−339	407	219	347	373	339	−375	390	366	298	333	329
σ	13	20	42	33	24	22	29	27	22	52	23	13	7	18
1982 mean	−474	402	−352	433	216	364	357	353	−376	402	384	280	323	319
σ	30	27	43	33	17	11	47	22	32	44	30	20	8	11

TABLE 5

Radial Velocities of Br 18 (WN9)

JD-2,440,000	He Ia 3819 .606	He Ia 3888 .646	He Ie 3888 .646	N IIIe 3994 .996	He Ia 4026 .189	He Ie 4026 .189	Si IVe 4088 .863	N IIIa 4097 .31	Hδe 4101 .737	Si IVe 4116 .104	Hγe 4340 .468	He Ia 4471 .507	He Ie 4471 .507	N IIIe 4634 .16	N IIIe 4641 .27	He IIe 4685 .682	He Ia 4713 .143	He Ie 4713 .143	Hβe 4861 .332
3839.612	−90	−144	284	258	−39	314	280	+6	327	201	260	−91	291	209	190	202	−50	278	245
3840.613	−59	−147	283	208	−55	306	250	−25	323	202	264	−118	275	193	199	208	−39	280	245
3841.685	−84	−135	301	252	−61	315	229	−5	336	222	264	−87	287	180	201	212	−63	293	240
3842.608	−105	−143	292	248	−72	327	284	−10	347	210	266	−98	299	194	197	207	−28	294	245
3843.607	−129	−132	288	243	−55	308	255	+4	353	210	256	−106	281	220	284	202	−82	290	236
3844.603	−63	−156	276	291	−58	321	279	−16	333	211	261	−89	288	209	213	207	−25	290	235
3845.619	−102	−132	284	253	−54	294	259	+15	323	249	261	−83	284	221	193	214	−72	249	237
3846.601	−93	−150	281	254	−33	291	248	+12	354	217	269	−85	292	203	129	208	−49	234	240
3847.617	−46	−138	291	189	−23	318	278	+22	365	243	269	−64	298	236	214	212	−61	259	255
4260.615	−115	−122	332	212	−60	346	277	+12	329	220	252	−60	309	206	179	202	−61	277	237
4261.606	−101	−167	272	247	−33	340	286	+22	348	234	264	−70	300	195	205	215	−54	279	230
Mean	−90	−142	289	241	−49	316	266	+3	340	220	262	−86	291	206	198	208	−53	275	240
σ	25	13	16	28	15	17	19	16	14	16	5	17	10	16	11	5	18	20	7
1978 mean ...	−86	−142	287	244	−50	310	262	0	340	218	263	−91	288	207	199	208	−52	274	242
σ	26	8	7	30	15	12	19	15	15	17	4	15	8	17	10	4	19	22	6
1980 mean ...	−108	−144	302	230	−46	343	282	+17	338	227	258	−65	304	200	192	208	−58	278	234
σ	10	32	42	25	19	4	6	7	13	10	8	7	6	8	18	9	5	1	5

TABLE 6

RADIAL VELOCITIES OF Br 26 (WN7)

JD- 2,440,000	Phase[a]	He I*a* 3888.646	N IV*e* 4057.759	Hδ*e* 4101.737	He II*e* 4199.83	Hγ*e* 4340.468	He II*e* 4541.59	N III*e* 4638	He II*e* 4685.682	Hβ*e* 4861.332
4254.729.....	0.213	−1194	431	370	547	485	538	313	328	355
4255.658.....	0.700	−1022:	−10	42	55	30	78	169	233	42
4256.691.....	0.242	−1173	468	363	495	459	435	339	301	327
4257.629.....	0.733	−1122:	−70	−41	4	4	95	31	219	52
4258.685.....	0.287	−979	418	417	467	476	493	320	335	333
4259.644.....	0.790	−1034	−32	−36	113	12	152	45	188	0
4260.660.....	0.322	−1248	401	378	394	437	490	361	378	401
4261.653.....	0.843	−1078	2	−13	128	30	88	50	156	37
4262.690.....	0.387	−1215	332	337	474	424	400	374	383	269
4586.546.....	0.167	−1551	372	283	520	406	...	274	302	382
4587.816.....	0.833	−1019	−17	−7	8	−68	48	15	172	56
4588.549.....	0.217	−1012	411	413	503	...	...	418	345	507
4594.714.....	0.449	−1191	203	...	497	391	340	330	431	353
4595.813.....	0.025	−1012	197	139	475	406	244	17	196	219
4597.817.....	0.076	−1138	246	226	525	467	339	226	260	371
4598.818.....	0.601	−1025	44	99	169	−4	228	265	274	266
4979.612.....	0.230	−1248	387	413	500	482	553	321	337	447
4980.539.....	0.716	−881	−54	−18	18	−81	−12	99	191	63
4980.831.....	0.869	...	48	−114	32	−57	6	38	155	43

NOTE: Balmer line rest wavelengths are used for Hδ, γ, β, although Pickering He II emission contribute significantly to these lines.
[a] Phase zero at JD 2,444,256.23 + 1.9075E (from N IV*e*).

Figure 3*c* shows that the P Cygni absorption component of He I 3888 displays low-amplitude variability nearly in antiphase with the variation in RV of N IV 4058. This metastable He line is probably formed relatively far out in the wind and does not participate in the orbital motion.

Note that Br 26 has relatively broad emission lines for its spectral subclass; e.g., N IV 4058 (FWHM $\sim$ 9 Å) is $\sim$twice as broad in Br 26 as in most other WN6,7 stars observed in the LMC (typical FWHM $\sim$ 4–5 Å), except Br 72 = R130, which is an exceptionally broad line star. Could this be due to rotational broadening as a result of spin-orbit synchronization in a short-period binary? This appears unlikely, since excessively high rotation ($v \gtrsim 10^3$ km s^{-1}) of the wind itself is required in order to compete with the high wind ejection speed. Conservation of angular momentum (neglecting forced rotation by a magnetic field) would lead to even higher rotation speeds of the central star.

Figure 3*d* shows the phase-dependency of the width and strength of He II 4686 from the IDS data. The variations appear to be real: the star Br 90, with similar spectrum (WN7, in which He II 4686 has FWHM $\sim$17 Å, $W_e = -66.3 \pm 0.3(\sigma)$ Å from three IDS spectra of similar quality), shows no significant variations, even though it is also a binary, but of long period (see Table 1). In Figure 3*d*, He II 4686 appears to be $\sim$30% weaker than the continuum and narrower at orbital phase (from N IV 4058) $\sim$0.5 when the W-R component is behind. Presumably part of its wind is eclipsed at this time, such that the emission regions are more affected than the (smaller) continuum regions, by the massive (probably O-type) companion, which is not seen in the combined spectrum.

Such a companion star is also manifested in Figure 3*e*, which shows a continuum light curve (Table 9), obtained in 1980 December on the CTIO 0.6 m telescope. The light curve shows a cusplike dip of amplitude $\Delta V \sim 0.065$ mag at orbital phase zero, when the O star is behind and its light is dispersed most by the free electrons in the W-R wind. There is no indication of

TABLE 7

IDS DATA FOR Br 26

JD 2,440,000	N IV Phase	RV N IV 4057.759	He II 4686 Phase	RV He II 4685.682	He II 4686 W_e (Å)	FWHM (Å)
5311.594.....	0.271	351	0.134	404	−101.2	22.6
5312.656.....	0.828	−56	0.691	180	−99.9	19.9
5314.699.....	0.899	25	0.762	206	−105.0	21.7
5315.662.....	0.403	203	0.267	468	−86.2	18.7

TABLE 8

CIRCULAR ORBIT SOLUTIONS FOR Br 26 (WN7)

Quantity	He II*e* 4685.682	N IV*e* 4057.759	Mean Hδ, γ, β Emission	N III 4638	Mean He II*e* 4199.83/4541.59
Period (d)			1.9075 ± 0.0002 (s.e.m.)		
γ(km s^{-1})	273 ± 5	182 ± 6	213 ± 9	208 ± 11	284 ± 11
K(km s^{-1})	113 ± 8	213 ± 8	222 ± 11	179 ± 16	232 ± 14
E_0-JD 2,444,250	6.49 ± 0.02	6.23 ± 0.02	6.27 ± 0.02	6.45 ± 0.03	6.24 ± 0.03
σ(km s^{-1})	22	26	37	44	47

NOTE.—The IDS data were not included in these fits.

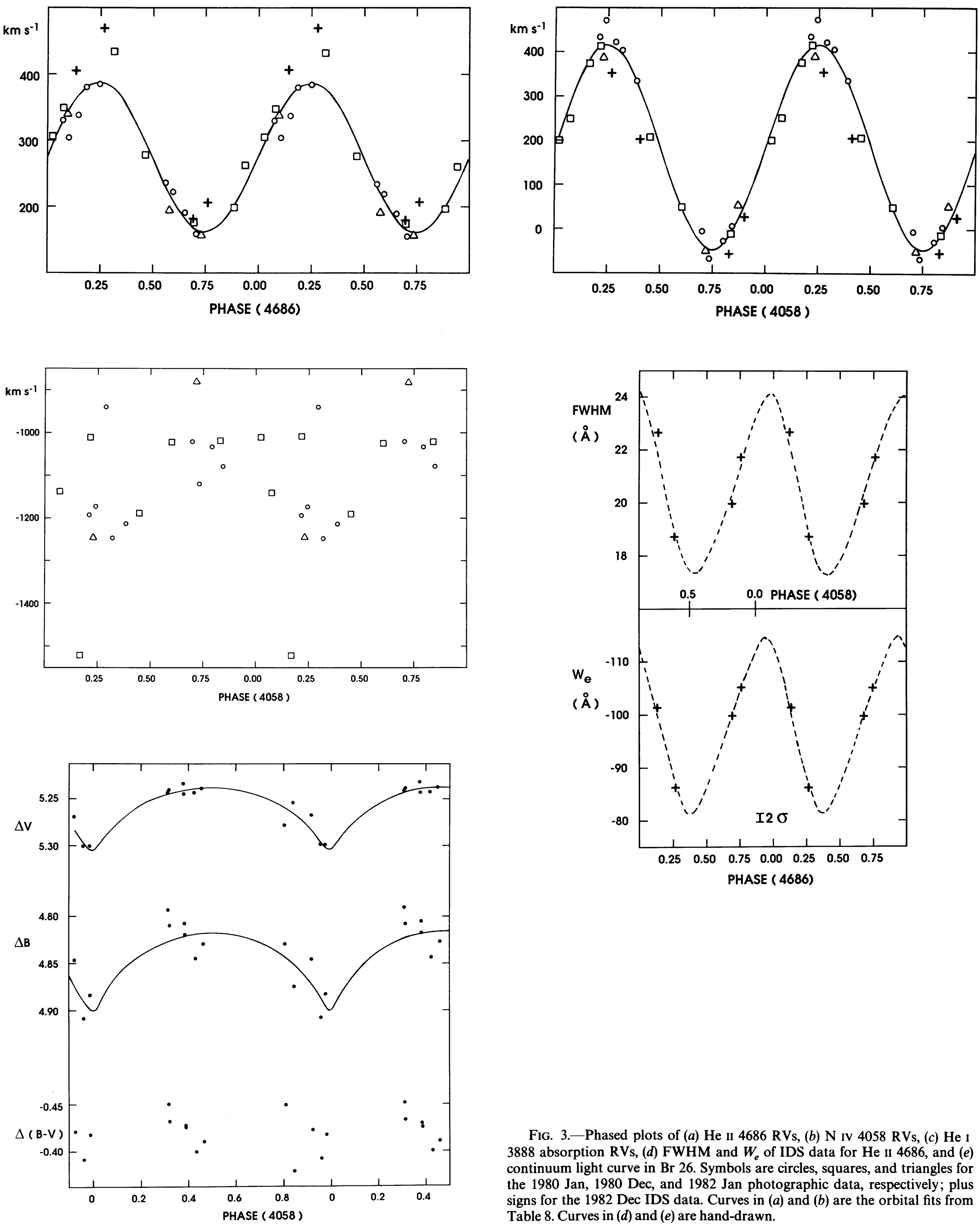

FIG. 3.—Phased plots of (*a*) He II 4686 RVs, (*b*) N IV 4058 RVs, (*c*) He I 3888 absorption RVs, (*d*) FWHM and W_e of IDS data for He II 4686, and (*e*) continuum light curve in Br 26. Symbols are circles, squares, and triangles for the 1980 Jan, 1980 Dec, and 1982 Jan photographic data, respectively; plus signs for the 1982 Dec IDS data. Curves in (*a*) and (*b*) are the orbital fits from Table 8. Curves in (*d*) and (*e*) are hand-drawn.

TABLE 9

PHOTOMETRY OF Br 26

JD-2,440,000	PHASE[a]	WR-C1 ΔV	WR-C1 ΔB	WR-C1 $\Delta(B-V)$	C2-C1 ΔV	C2-C1 ΔB	C2-C1 $\Delta(B-V)$
4590.647.....	0.317	5.244	4.793	−0.451	3.820	4.294	0.474
4590.785.....	0.389	5.247	4.819	−0.428	3.821	4.302	0.481
4591.588.....	0.810	5.280	4.831	−0.449	3.817	4.289	0.472
4592.567.....	0.323	5.242	4.810	−0.432	3.837	4.294	0.452
4592.689.....	0.387	5.234	4.808	−0.426	3.826	4.300	0.474
4592.776.....	0.433	5.245	4.846	−0.399	3.822	4.298	0.476
4592.839.....	0.466	5.240	4.829	−0.411	3.853	4.333	0.480
4593.565.....	0.847	5.255	4.876	−0.379	3.853	4.305	0.452
4593.711.....	0.923	5.269	4.847	−0.422	3.840	4.287	0.447
4593.787.....	0.963	5.300	4.908	−0.392	3.824	4.305	0.481
4593.826.....	0.983	5.300	4.883	−0.417	3.835	4.309	0.474
Mean		5.262	4.841	−0.419	3.832	4.301	0.470
σ		0.024	0.036	0.022	0.013	0.013	0.012

[a] W-R in front at phase 0: JD 2,444,256.23 + 1.9075E. The comparison stars C1, C2 are located $\sim 5'.5$ and $6'$, respectively, north of Br 26.

a real eclipse of the stars themselves. This light curve is very similar to the Galactic WN7 SB1 star WR 148 (Moffat and Shara 1986).

Br 26 is surrounded by an arc-shaped H II nebulosity, presumably a result of interaction of the stellar wind with the interstellar medium. No nebular emission lines are seen, however, in the present spectra.

d) Br 65, WN7

There has been some confusion in the classification of this star in the past, because it is located in a very crowded area. Lortet and Testor (1988) show the proper identification (based on this work) and give a revised (fainter!) magnitude. The present spectra were obtained with the correct star clearly separated from its close (separation $\sim 3''$–$5''$) visual companions. Nevertheless, Br 65 appears to consist of two stars of similar magnitude, separated by $\lesssim 1''$. This probably explains the somewhat diluted nature of the spectral emission lines compared to other WN7 stars.

Table 10 shows that Br 65 is another SB1. A period of $3^d.0032 \pm 0^d.0002$ is obtained, from which orbital solutions for the strongest lines are given in Table 11 and shown in Figure 4 for two lines. Again, as for Br 26, the emission line of N IV 4058 probably best reflects the orbit of the W-R component; He II 4686 and N III 4638 show reduced amplitudes and are phase-shifted.

In this star, the upper Balmer lines are seen in absorption. They probably originate partly in the unresolved visual companion (separation $\lesssim 1''$), which also dilutes the emission-line spectrum (cf. Fig. 2). However, their velocities do follow those of the emission lines, but with reduced amplitude (due to blending) and strongly negative systemic velocities. It is not uncommon to see intrinsic, violet-shifted photospheric absorption lines in WN7 stars.

The P Cygni absorption lines of He I show no phase dependency, as was found for Br 26. They are thus likely formed far out beyond the orbit.

The interstellar nebular lines show constant RV and reflect the high degree of reliability and stability of the spectrograph (cf. Table 10).

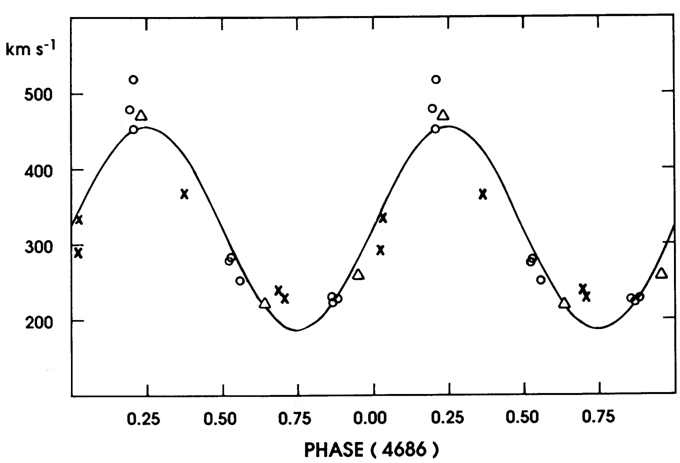

FIG. 4*a*

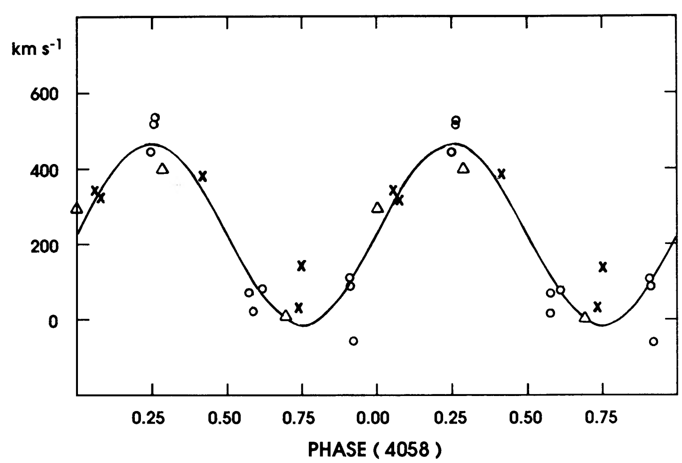

FIG. 4*b*

FIG. 4.—Orbital data and fits for (*a*) He II 4686 and (*b*) N IV 4058 in Br 65. Symbols are crosses, circles, and triangles for 1978 Dec, 1980 Jan, and 1982 Jan, respectively.

TABLE 10

RADIAL VELOCITIES OF Br 65 (WN7)

JD-2,440,000	Phase[a]	H10a 3797.900	H9a 3835.386	He Ia 3888.646	He Ia 4026.189	N IVe 4057.759	Hγa 4340.468	N IIIe 4638	He IIe 4685.682
3843.746.....	0.746	106	170	−187	−169	133	−10	21	227
3844.712.....	0.067	125	209	−368	−43	333	+2	173	288
3845.743.....	0.411	454	189	−354	+100	375	+60	299	363
3846.717.....	0.735	120	−125	−277	−159	28	−104	−2	234
3847.738.....	0.075	161	270	−349	228	329	+54	260	331
4254.772.....	0.608	44	41	−469	−93	75	−109	82	248
4255.689.....	0.941	19	101	−506	−225	87	−42	34	218
4256.721.....	0.257	194	185	−405	−12	515	+68	271	450
4257.683.....	0.578	−121	−90	−535	−216	68	−32	79	278
4258.714.....	0.921	94	38	−626	−403	−62	−6	109	222
4259.688.....	0.245	...	321	−410	142	439	+156	160	475
4260.686.....	0.578	−69	130	−387	−56	15	−57	144	279
4261.679.....	0.908	192	59	−299	−322	105	−78	94	221
4262.729.....	0.258	−70	...	−473	−25	521	+103	284	515
4980.568.....	0.282	...	178	−424	−75	392	+138	396	467
4981.797.....	0.692	140	21	...	−213	1	−149	149	216
4982.728.....	0.002	126	−230	−306	−55	289	−58	119	256

Interstellar Means

Date	[O II]e 3727.55	Ca II-Ka 3933.664	Hβe 4861.332
1978.....	294 ± 7(16)	176 ± 7(15)	264 ± 10(22)
1980.....	289 ± 13(38)	146 ± 21(62)	260 ± 5(14)
1982.....	276 ± 17(29)	69 ± 39(67)	257 ± 13(18)

NOTES.—H9, 10, 11 and 12 behave like Hγ, although they become progressively noisier: H8 and Hε show reduced amplitude, due to blending. Errors of the interstellar RVs are errors of the mean and in parentheses standard deviations.

[a] Phase zero occurs at JD 2,443,844.51 + 3.0032E.

e) Br 73, WN7

This object consists of ∼four stars of similar magnitude that are inseparable on the 2″ wide slit used. It is assumed that only one of the stars is actually W-R. This was confirmed and refined very recently by Testor, Llebaria, and Debray (1988). As for Br 65, the resulting W-R spectrum consequently appears strongly diluted (cf. Fig. 2).

RVs (Table 12) of the best emission line (He II 4686) show a dispersion of $\sigma = 24$ km s^{-1} about a simple mean value. This is much like the O-C dispersion for the same line in Br 26 and Br 65. A formal period search of the λ4686 RVs yields the best period $P = 7^{\mathrm{d}}.9145$, with longer periods also possible, and $K = 27 \pm 5$ km s^{-1}, σ(O-C) = 11 km s^{-1}. None of these periods is considered real; thus, the star is taken to be single. Nebular emission lines are visible in the spectrum.

f) Br 75, WN7

Being close to the bright 30 Dor nebula, this star has a spectrum showing strong nebular lines, which prevent reliable measure of the RVs of many of the W-R lines, except for the relatively strong lines given in Table 13. These show that Br 75 is a constant RV, probably single star.

g) Br 86, WNL/Of

Because of the strong contamination by nebular emission lines and the weakness of the narrow, intrinsic lines, only He II 4686 gives relatively reliable RVs ($\sigma \sim 30$ km s^{-1} per group of data). RVs of He IIa 4199, 4541 and N IIIe 4638 are also derived; with $\sigma > 100$ km s^{-1} for the last two, they are not given. He IIa 4199 gives $\sigma \sim 80$ km s^{-1} per group (see Table 14).

TABLE 11

CIRCULAR ORBIT SOLUTIONS FOR Br 65 (WN7)

Quantity	He IIe 4685.682	N IVe 4057.759	Hγa 4340.468	N IIIe 4638	He Ia 4026.189
Period (d)	3.0032 ± 0.0002 (s.e.m.)				
γ (km s^{-1})	319 ± 8	223 ± 19	+1 ± 11	164 ± 15	−85 ± 30
K (km s^{-1})	134 ± 11	238 ± 25	105 ± 15	128 ± 21	152 ± 42
E_0-JD 2443840	4.65 ± 0.04	4.51 ± 0.05	4.53 ± 0.07	4.62 ± 0.08	4.64 ± 0.14
σ (km s^{-1})	31	71	41	57	120

TABLE 12

RADIAL VELOCITIES OF Br 73 (WN7)

JD-2,440,000	H9a 3835.051	H8a 3889.051	N IVe 4057.759	He Ia 4471.507	He IIe 4685.682
4254.825.....	312	321	323	210	327
4255.721.....	304	339	314	305	321
4256.750.....	369	190	284	...	303
4258.747.....	376	230	...	223	285
4259.742.....	378	...	...	218	264
4260.715.....	271	178	411	207	288
4261.713.....	285	249	208	259	290
4262.765.....	186	323	343	180	308
4974.790.....	128	...	311	283	299
4977.671.....	293	245	378	249	285
4979.728.....	310	253	...	234	244
4982.753.....	309	201	139	188	317
Mean.....	285	253	301	232	294
σ..........	69	58	83	39	24

Interstellar Means

Date	[O II]e 3727.55	Ca II-Ka 3933.664	Hβe 4861.332	[O III]e 4959
1980.....	282 ± 8(22)	174 ± 16(46)	246 ± 4(11)	265 ± 4(12)
1982.....	266 ± 9(18)	163 ± 10(19)	251 ± 7(15)	268 ± 11(22)

NOTE.—Errors of interstellar lines as in Table 10.

Based on the 1978, 1980 data only, one would conclude that the RV of Br 86 is constant. However, including the data from 1982 shows a clear, long-term variation. A period search yields many discrete possibilities, with $P = 52^{d}.7$ marginally the best. Absorption and emission lines move in phase (cf. Table 15 and Fig. 5).

h) Br 89, WN7

The nebular emission lines are relatively strong in this 30 Dor region star, although less so than in Br 87 = R140. He I 3888 shows a ~ 800 km s^{-1} blueshifted, weak P Cygni absorption profile, although it may be partly contaminated by the nearby interstellar nebular emissions of [Ne III] 3868 and He I 3888. N V 4603–4619 also shows P Cygni profiles. The RVs show no indication of significant variability over the 3-year interval (Table 16); hence Br 89 is probably single.

i) Br 90, WN7

This star is also located in the 30 Dor area and has a spectrum almost identical to that of Br 89. However, its strongest and most reliably measured W-R emission lines (N IV 4058 and He II 4686) show significant variability in RV (see Table 17). A period search yields several discrete periods, of which the best is $P = 25^{d}.17$. The N III 4638 line does not appear to vary like the other two lines. An orbit fit is given in Table 18 and shown in Figure 6.

j) Br 91, WN9

The spectrum of this star is very much like that of the WN9 star Br 18. It also shows no evidence for binary motion (Table 19).

k) Br 92, WN6

The data in Table 20 indicate that this star probably does not vary in RV. In any case, a formal period search yields a combined best period for the two best lines, N IV 4058 and He II 4686, of $P = 26^{d}.52$. The RV amplitude with this period is $K = 13 \pm 5$ km s^{-1} for each of the lines, which do vary in phase. However, this result is marginal and Br 92 is considered to be a single star.

TABLE 13

RADIAL VELOCITIES OF Br 75 (WN7)

JD-2,440,000	N IVe 4057.759	N IIIe 4638	He IIe 4685.682
3839.779	204	214	295
3840.779	199	168	266
3842.767	229	260	274
3843.787	195	186	279
3844.754	212	241	290
3845.783	188	200	302
3846.761	222	165	283
3847.788	190	180	280
4260.829	214	248	296
4261.783	186	242	302
Mean	204	210	287
σ	15	35	12
1978 mean	205	202	284
σ	15	34	12
1980 mean	200	245	299
σ	20	4	4

Interstellar Means

Date	[O II]e 3727.55	[Ne III]e 3868.700	H8e 3889.051	Ca II-Ka 3933.664	Hϵe 3970.074	Hδe 4001.737	Hγe 4340.468	Hβe 4861.332
1978.....	286 ± 5(15)	268 ± 3(8)	260 ± 4(11)	236 ± 11(32)	258 ± 7(20)	261 ± 4(10)	254 ± 2(5)	253 ± 2(5)
1980.....	278 ± 5(7)	254 ± 5(6)	250 ± 8(11)	228 ± 46(66)	234 ± 32(45)	268 ± 2(4)	264 ± 4(5)	242 ± 2(4)

NOTE.—Errors of interstellar lines as in Table 10.

TABLE 14

RADIAL VELOCITIES OF Br 86 (WNL/Of)

JD-2,440,000	He II 4685.682	He IIa 4199.830	JD-2,440,000	He II 4685.682	He IIa 4199.830
3838.835	340	256	4974.819	111	188
3839.800	267	335	4975.819	194	134
3840.819	290	341	4976.825	179	320
3842.790	261	376	4978.775	197	253
3843.826	260	337	4979.747	189	...
3844.785	311	181	4980.798	192	42
3845.827	282	259	4982.818	237	199
3846.782	294	282	Mean	259	275
3847.838	262	348	σ	56	88
4255.764	287	278	1978 mean	285	302
4256.807	305	160	σ	27	62
4257.785	268	354			
4258.815	294	321	1980 mean	294	310
4259.777	275	320	σ	21	68
4260.774	281	369			
4261.802	307	306	1982 mean	186	189
4262.836	332	368	σ	38	96

Interstellar Means

Date	[O II]e 3727.55	[Ne III]e 3868.700	H8e 3889.051	Ca II-Ka 3933.664	Hϵe 3970.074	Hδe 4101.737	Hγe 4340.468	Hβe 4861.332
1978	289 ± 5(14)	276 ± 4(11)	260 ± 2(6)	218 ± 9(26)	240 ± 8(23)	268 ± 2(6)	260 ± 1(3)	256 ± 1(4)
1980	275 ± 4(10)	278 ± 3(7)	272 ± 8(22)	192 ± 20(58)	262 ± 10(28)	274 ± 3(8)	272 ± 2(4)	253 ± 2(6)
1982	275 ± 6(15)	260 ± 7(18)	262 ± 3(7)	182 ± 19(52)	252 ± 8(16)	265 ± 4(10)	262 ± 3(7)	259 ± (2)

NOTE.—Errors of interstellar lines as in Table 10.

V. GENERAL DISCUSSION

a) Absolute Magnitudes

Figure 7 shows an M_v histogram of all the known LMC WNL stars from Table 1, divided into WN6,7 and WN8,9. Table 21 (omitting Br 72 in which the supergiant companion dominates; Br 82, the crowded core of 30 Dor; Br 86 as a nonpure W-R; and Br 87 which is crowded) bears out the obvious point of Figure 7: both groups of stars overlap considerably in intrinsic brightness, with the mean of the whole LMC sample of WN8,9 stars being only 0.5 ± 0.4 mag fainter than the WN6,7 stars. This difference is barely significantly different from zero. This is especially so if one realizes that WN6,7 stars are more often binaries, and tend to be found more frequently than WN8,9 stars in very crowded regions (e.g., 30 Dor), where their absolute magnitudes tend to be overestimated. Some attempt has been made to correct for this crowding effect, but it is probably on the conservative side. Indeed, the WN6,7 stars outside 30 Dor are no brighter than the WN8,9 stars, possibly for this reason, although one cannot yet exclude the possibility that the 30 Dor stars are slightly brighter intrinsically. In this paper, it will be assumed that both

TABLE 15

CIRCULAR ORBIT SOLUTIONS FOR Br 86 (WNL/Of)

Parameter	He IIe 4685.682	He IIa 4199.83
Period (d)	52.7	
γ (km s^{-1})	233 ± 7	251 ± 20
K (km s^{-1})	67 ± 9	66 ± 19
E_0-JD 2,443,800	78.5 ± 1.5	83.5 ± 4.9
σ (km s^{-1})	24	70

TABLE 16

RADIAL VELOCITIES OF Br 89 (WN7)

JD-2,440,000	N IVe 4057.682	N IIIe 4638	He IIe 4685.682
3838.818	204	165	275
3839.853	219	217	273
3840.846	175	288	263
3841.835	184	113	238
3842.844	218	236	254
3843.840	206	216	270
3844.838	183	261	288
3846.835	244	142	266
3847.853	187	132	279
4260.861	200	183	266
4261.855	198	159	242
4975.542	180	223	278
4976.813	168	300	274
Mean	197	203	267
σ	21	60	14
1978 mean	202	197	267
σ	22	61	15
1980 mean	199	171	254
σ	1	17	17
1982 mean	174	262	276
σ	8	54	3

Interstellar Means

Date	[O II]e 3727.55	Ca II-Ka 3933.664	Hγe 4340.468	Hβe 4861.332
1978	281 ± 9(26)	213 ± 17(50)	329 ± 9(27)	269 ± 6(17)
1980	291 ± 14(20)	217 ± 68(97)	347 ± 25(35)	253 ± 4(6)
1982	333 ± 10(14)	188 ± 32(46)	334	262 ± 3(4)

NOTE.—Errors of interstellar lines as in Table 10.

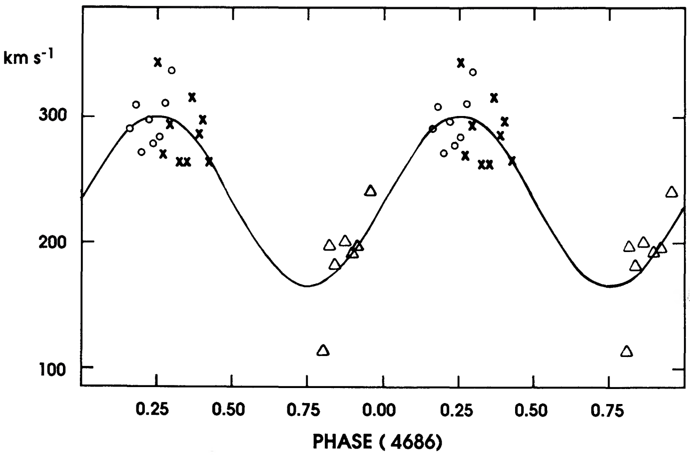

FIG. 5a

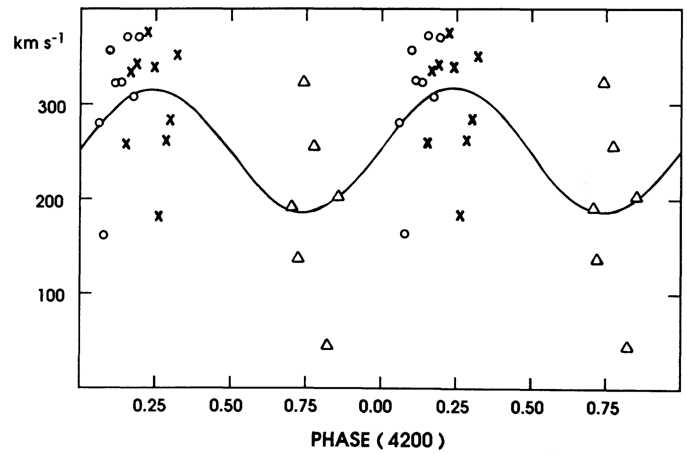

FIG. 5b

FIG. 5.—Orbital data and fits for (*a*) He II 4686 emission and (*b*) He II absorption in Br 86. Symbols are crosses, circles, and triangles for 1978 Dec, 1980 Jan, and 1982 Jan, respectively.

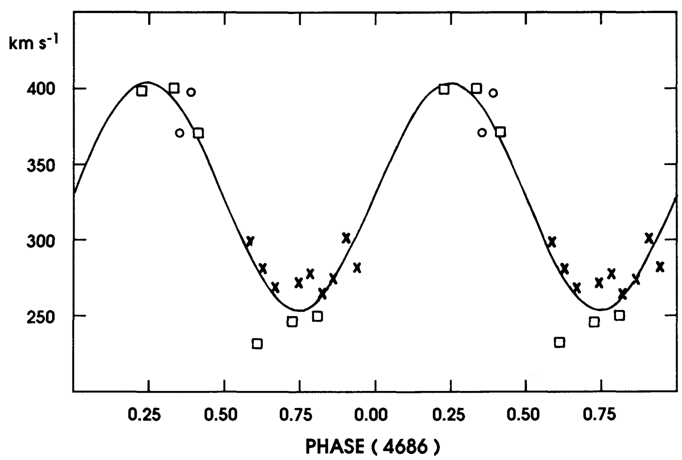

FIG. 6a

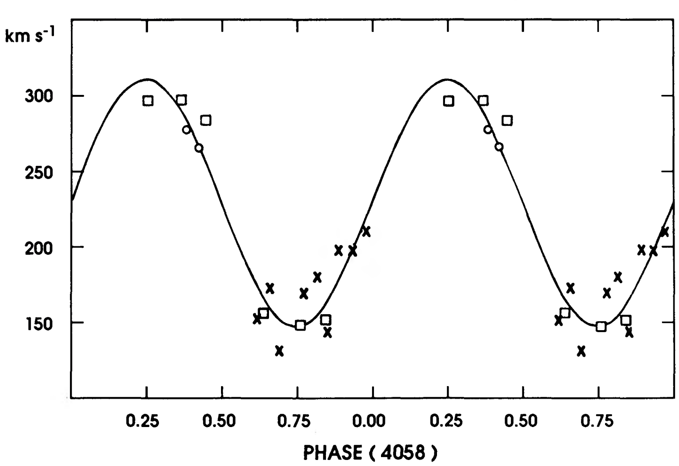

FIG. 6b

FIG. 6.—Orbital data and fits for (*a*) He II 4686 and (*b*) N IV 4058 in Br 90. Symbols are crosses, circles, and squares for 1978 Dec, 1980 Jan, and 1980 Dec, respectively.

groups are about equally bright, with $M_v \simeq -5.9$. The scatter for either group appears to be similar and relatively large, $\sigma(M_v) \sim 0.8$–0.9 mag.

b) *Binary Frequency*

Figure 7 shows that, among those LMC WNL stars looked at for binary RV variations, there is no significant selection effect regarding magnitude (one might have expected to find more binaries among the brighter stars; in fact the opposite is true, if anything). This probably implies that the (presumably O-type) companions are in general much less luminous and are drowned out by the bright W-R component. This also explains why WNL binaries are nearly all SB1, rarely SB2 (this may change in the future with higher S/N studies).

Figure 8 shows an *apparent* visual magnitude histogram (absolute magnitudes are not known for most Galactic stars) of

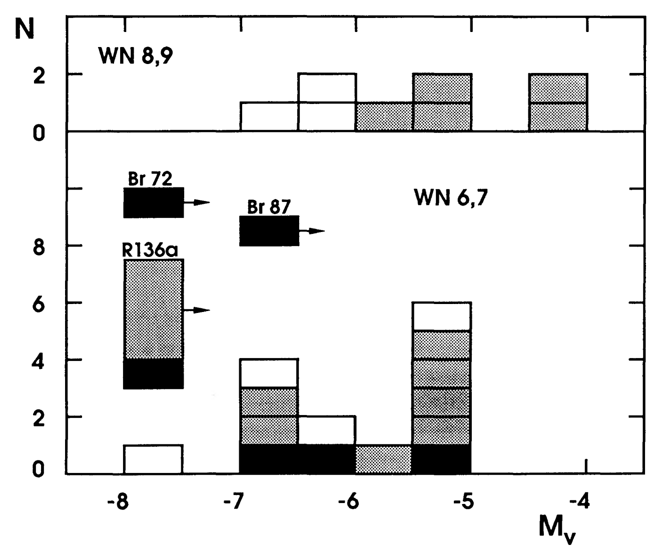

FIG. 7.—Frequency of LMC WNL stars divided into two groups as a function of absolute visual magnitude. Filled, hatched, and open areas refer to SBs, stars with no binary information, and stars with constant RV, respectively.

TABLE 17

Radial Velocities of Br 90 (WN7)

JD-2,440,000	N IVe 4057.759	N IIIe 4638	He IIe 4685.682
3838.781	152	312	296
3839.833	172	263	280
3840.801	131	229	267
3842.826	169	254	270
3843.809	179	307	276
3844.822	143	258	263
3845.808	197	202	273
3846.818	198	282	300
3847.812	210	272	280
4260.807	277	255	369
4261.838	266	312	395
4584.835	296	299	397
4587.643	296	280	398
4589.594	283	275	369
4594.582	155	173	230
4597.543	146	262	244
4599.541	151	256	248
Mean	201	264	303
σ	59	37	58
1978 mean	172	264	278
σ	27	35	13
1980.1 mean	272	284	382
σ	8	40	18
1980.9 mean	221	258	314
σ	77	44	82

Interstellar Means

Date	[O II]e 3727.55	Ca II-Ka 3933.664	Hγe 4340.468	Hβe 4861.332
1978	291 ± 6(19)	240 ± 11(32)	308 ± 9(27)	287 ± 3(10)
1980.1	297 ± 6(8)	252 ± 20(29)	308 ± 18(25)	277 ± 7(10)
1980.9	308 ± 17(41)	207 ± 22(53)	284 ± 13(31)	286 ± 4(9)

Note.—Errors of interstellar lines as in Table 10.

the Galactic WNL stars from Table 2. Again, we see no significant selection effect favoring detection of binaries among the brighter stars (the opposite appears to be true if anything).

Table 22 compares the binary frequency of WN8,9 versus WN6,7 stars in the LMC and in the Galaxy (there is no significant difference between WN6 and WN7, or between WN8 and WN9). This reveals the striking result that there are no WN8,9 + O binaries, while the WN6,7 stars show a relatively high frequency of W-R + O binaries in both galaxies (57%). The overall binary frequency among WNL stars is 43%, like the overall W-R binary frequency (cf. Moffat *et al.* 1986).

c) *Masses*

From Table 1 we see that there are six single-line, massive binaries (SB1) among the bona fide LMC WNL stars (i.e., neglecting Br 86). There are no double-line binaries. Two of the SB1 are located in extremely crowded areas (Br 82 in the 30 Dor core and Br 87 in R140), with other W-R stars; their RV orbits are too strongly perturbed to be useful. The remaining four systems (Br 26, 65, 72, 90) yield a mean mass function $f(m) \equiv (M_O \sin i)^3/(M_{W\text{-}R} + M_O)^2 = 3.0 \pm 1.3(\sigma)\ M_\odot$. As it turns out, the WNL/Of star Br 86 also has a value of $f(m)$ in this range. Allowing for the dilution effect of several W-R components in R136 and R140 leads to reasonable $f(m)$'s for them as well.

TABLE 18

Circular Orbit Solution for Br 90 (WN7)

Parameter	N IVe 4057.759	He IIe 4685.682
Period (d)	25.17	
γ (km s^{-1})	229 ± 5	327 ± 5
K (km s^{-1})	82 ± 7	75 ± 7
E_0-JD 2,443,800	48.4 ± 0.3	49.2 ± 0.4
σ (km s^{-1})	16	18

From Table 2, we find listed eight WNL binaries with massive companions and relatively unperturbed orbits (WR 12, 22, 47, 138, 141, 145, 153, and 155), neglecting the possible double W-R binary WR 8; WR 43, which contains several W-R stars; and WR 148 which has an extraordinarily low mass function. All are of type WN6,7 while three are SB2's (WR 47, 138, and 153). These eight stars yield a mean $f(m) = 6.8 \pm 3.9\ (\sigma)\ M_\odot$. Omitting the three SB2's, which tend to have higher $f(m)$'s, since the W-R component in those cases is less luminous and thus less massive than in SB1's, gives $f(m) = 4.9 \pm 2.2(\sigma)\ M_\odot$. The latter value is only slightly larger than the corresponding LMC value (SB1's only). The difference could be due to a systematic difference in orbital inclination between the two galaxies. Neglecting this possibility, and adopting an overall mean $f(m) = 4.0\ M_\odot$ for WNL stars and a typical orbital inclination in a random sample, $i \simeq 60°$, yields $M(\text{WNL}) \simeq 36\ M_\odot$ for an average O star of $M(\text{O}) \simeq 30\ M_\odot$ [$M(\text{WNL}) = 62\ M_\odot$ for $M(\text{O}) \simeq 40\ M_\odot$]. These values are in the range of those obtained for the well-determined SB2 system WR 47 (Moffat *et al.* 1989): $M(\text{WN6}) = 48 M_\odot$, $M(\text{O5 V}) = 57\ M_\odot$. The corresponding mean mass ratio $M(\text{WNL})/M(\text{O}) \simeq 1.2$ (1.6) is slightly greater than unity, as opposed to non–WNL stars, where it is generally below ~0.5. This agrees with the statement made in § I that the WNL phase is probably the first W-R phase before mass loss of the W-R component

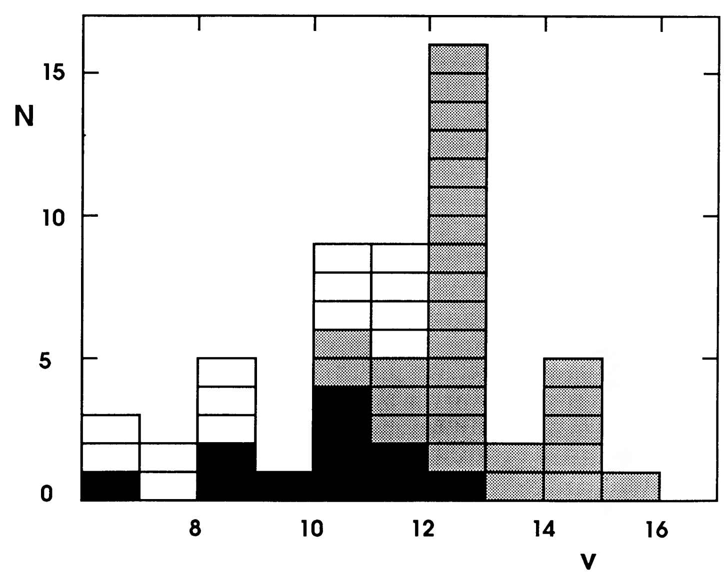

Fig. 8.—Frequency of Galactic WNL stars as a function of visual apparent magnitude. Filled, hatched, and open areas refer to SB2 or SB1 (including WR 8, 43, 138, 148); stars with no binary information; and stars with constant RV or SB1l (cf. Table 2), respectively.

TABLE 19

RADIAL VELOCITIES OF Br 91 (WN9)

JD-2,440,000	He Ia 3888.646	He Ie 3888.646	He Ia 4026.189	He Ie 4026.189	Si IVe 4088.863	N IIIa 4097.31	Hδe 4101.737	Si IVe 4116.104	Hγe 4340.468	He Ia 4471.507	He Ie 4471.507	N IIIe 4641.27	He IIe 4685.682	He Ie 4921.929	Hβe 4861.332
4255.803	−129	371	+5	388	219	31	403	316	317	−64	362	225	240	218	270
4256.790	−130	353	−21	390	220	5	418	250	319	−38	360	202	272	261	276
4258.793	−217	366	−31	398	312	21	406	245	321	−73	374	226	270	251	253
4259.828	−126	398	+1	396	257	−3	387	260	324	−37	345	199	275	244	270
4260.742	−185	334	+56	416	280	−11	419	294	308	−34	364	182	265	274	259
4261.747	−149	378	−24	390	281	32	410	259	309	−57	386	236	248	290	259
4262.797	−148	355	−56	379	325	30	424	266	321	−7	358	221	264	304	257
4586.826	−150	384	+100	...	220	−2	388	...	330	−36	383	214	271	304	282
4594.792	−166	350	−49	445	264	19	412	252	322	−71	343	182	265	226	281
Mean	−156	365	−2	400	264	14	407	268	319	−46	364	210	263	264	267
σ	30	20	51	21	40	17	13	25	7	22	15	20	12	32	11
1980.1 mean .	−155	365	−10	394	271	15	410	270	317	−44	364	213	262	263	263
σ	34	20	36	12	41	18	12	26	6	22	13	19	13	29	8
1980.9 mean .	−158	367	+26	445	242	8	400	252	326	−54	363	198	268	265	282
σ	11	24	105	...	31	15	17	...	6	25	28	23	4	55	1

Interstellar Means

Date	[O II]e 3727.55	[O III]e 4959
1980.1.....	265 ± 10(26)	262 ± 5(14)
1980.9.....	271 ± 10(14)	275

NOTE.—Some stellar RVs may be affected by nebular emission (e.g., He Ie 3888, Hδ, γ, β emis.). Errors of interstellar lines as in Table 10.

TABLE 20

RADIAL VELOCITIES OF Br 92 (WN6)

JD-2,440,000	He I a 3888.646	N IV e 4057.759	He II e 4199.830	He II e 4541.590	He II e 4685.682
4585.840	−870	191	482	410	338
4586.803	−853	195	558	361	330
4587.661	−791	168	452	405	350
4588.801	−938	193	451	380	322
4595.669	−784	207	541	298	358
4596.801	−785	196	503	442	366
4598.707	−958	184	406	388	348
4599.768	−875	226	433	390	365
4975.749	−975	214	299	451	357
4977.737	−844	219	394	403	351
4978.654	−885	193	433	350	345
4979.828	−993	194	367	406	335
4982.778	−881	204	431	398	339
Mean	−879	199	442	391	346
σ	70	15	70	39	13
1980 mean	−857	195	478	384	347
σ	68	17	53	42	16
1982 mean	−916	205	385	402	345
σ	65	12	55	36	9

Interstellar Means

Date	[O II]e 3727.55	Ca II-Ka 3933.664	Hγe 4340.468	Hβe 4861.332	[O III]e 4959	[O III]e 5007
1980	276 ± 7(20)	230 ± 30(85)	278 ± 5(14)	275 ± 2(7)	264 ± 3(8)	271 ± 8(22)
1982	246 ± 10(23)	183 ± 15(30)	284 ± 6(13)	278 ± 8(19)	258 ± 3(7)	257 ± 5(12)

NOTE.—Errors of interstellar lines are as in Table 10.

becomes significant compared to its originally lower mass companion.

d) *Line Widths and Systemic Velocities*

Figure 9 shows that the systemic RV of the strongest line (He II 4686) for LMC WNL stars increases with the width of the line. Rotation of the LMC is not important in this context, since there is large scatter even among the 30 Dor stars. With mean heliocentric RV for interstellar matter in the LMC of $\sim$270 km s^{-1} (Morgan and Böhm-Vitense 1988), Figure 9 shows that this line best reflects the true systemic RV only in narrow-line stars.

Figure 10 reveals a relatively tight correlation between the widths of the two best emission lines, N IV 4058 and He II 4686. On average, the N IV line is about half as broad as the He II line. Note that while WN9 stars clearly have the narrowest lines, the WN8 star is close to the lower limit of the WN6,7 stars, which tend to blend together. The violet absorption edge of He I 3888 is also least blueshifted for WN9 stars.

Finally, Figure 11 shows that the N IV line has a γ-velocity which is $\sim$100 km s^{-1} less on average than that for the He II line. This is compatible with Figure 9 for the He line alone, i.e., a narrower line shows reduced γ-velocity which is generally slightly more negative, while He II is much more positive than the true γ-velocity.

e) *The WN6,7–WN8,9 Dichotomy*

In § II, the distribution was noted between WN6,7 and WN7,8 stars. A more extensive, updated comparison is given in summary form in Table 23. The salient feature of this table is that, while these two subgroups are similar in luminosity and (probably) mass, the WN8,9 stars tend to have slower winds and larger core radii, are more variable, and tend to be runaway, non–W-R + O binaries.

TABLE 21

ABSOLUTE VISUAL MAGNITUDES (LMC)

Type	No. Stars	M_v ± s.e.m.	σ
WN9	4[a]	−5.8 ± 0.5	1.0
WN8	4	−5.3 ± 0.4	0.8
All WN8/9	8	−5.6 ± 0.3	0.9
WN8/9, 30 Dor	1	−5.4	
WN8/9, outside 30 Dor	7	−5.6 ± 0.4	1.0
WN7	9	−6.2 ± 0.3	0.9
WN6	5	−6.0 ± 0.3	0.7
All WN6/7	14	−6.1 ± 0.2	0.8
WN6/7, 30 Dor	10	−6.3 ± 0.3	0.8
WN6/7, outside 30 Dor	4	−5.6 ± 0.2	0.4

[a] Including Br 44a (WN8–9).

TABLE 22

W-R + O BINARY FREQUENCY OF WNL STARS STUDIED FOR RV VARIATIONS

Group	LMC	Galaxy	Sum
WN8,9	0/3 = 0.00	0/6 = 0.00	0/9 = 0.00 ± 0.33
WN6,7	5/9 = 0.56	11/19 = 0.58	16/28 = 0.57 ± 0.19
WN6–9	5/12 = 0.42	11/25 = 0.44	16/37 = 0.43 ± 0.17

NOTE.—Neglecting R136a but including HD 97950.

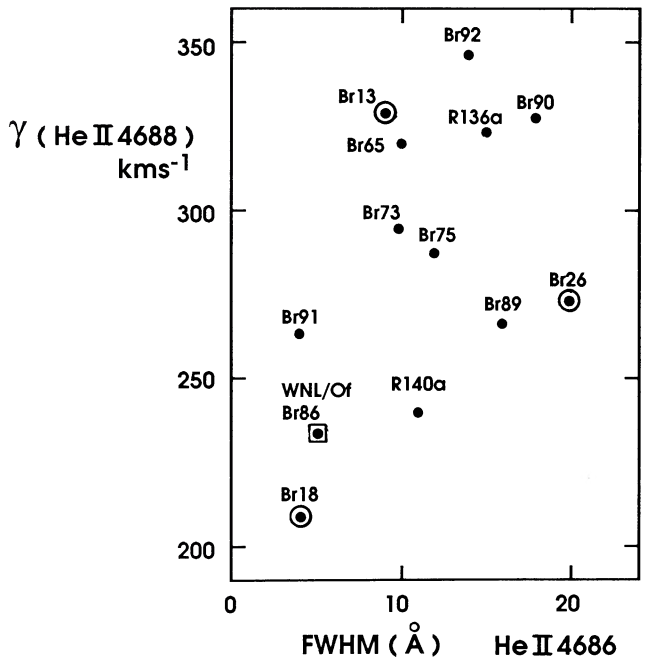

FIG. 9.—Systemic RV vs. line width for the He II 4686 emission line in the LMC WNL stars. Circled stars are located outside 30 Dor.

What is the source of this dichotomy? One possible hypothesis is that WN8,9 stars are the single (or W-R + c) *runaway* equivalents of WN6,7 stars. Both are formed (as are most stars) in clusters and associations, but WN8,9 stars are ejected via either of two conceivable processes: (1) dynamical interaction among the stars in the cores of young, dense stellar clusters, as suggested for the Population I OB-type runaway stars (Gies and Bolton 1986), although this may also work well for less dense clusters as well (Leonard and Duncan 1988), or (2) an impulsive kick from a supernova explosion in a binary system, resulting in a runaway W-R + c binary in most cases or a single runaway W-R star in other cases.

Process (1) would not readily explain the spectral difference between WN8,9 and WN6,7 stars (e.g., the runaway OB stars have similar spectra compared to non-runaway OB stars) and would not be compatible with the possible existence of binary WN8,9 + c systems, as suspected in the Galactic runaway WN8 stars WR 123 and WR 124 (see Moffat and Shara 1986). On the other hand, process (2) provides a fundamental difference, in that the WN8,9 component would be a *second* generation W-R star, compared to single or first generation WN6,7 stars. This could also give rise to differences in the spectra of these two subgroups, such as a more extended, H-rich envelope from mass accretion from the original primary star, further modified by a supernova explosion of the primary.

If (2) yields typical runaway speeds of ≈ 50 km s^{-1}, then in $\sim 5 \times 10^6$ yr ($\sim$ typical evolution time of a rejuvenated secondary before it enters the WNL stage), the star will have moved ~ 250 pc. This is ample distance to explain the dearth of WN8,9 stars in 30 Dor (one WN8,9 star relative to 16–17 WN6,7 stars) compared to the immediate vicinity of 30 Dor in the Shapley II association (number ratio of WN8,9 to WN6,7 stars: $7/17.5 = 0.4$, which is normal on a wide scale). Direct evidence for high peculiar RVs, whether due to (1) or (2), is difficult to extract from the observed systemic velocities (cf. Figs. 9 and 11).

The global number ratio of WN8,9 to all WNL stars is $\sim \frac{1}{4}$, which if (2) is correct, would imply that this same fraction of originally massive stars are binaries that end up as WN8,9 + c. Against hypothesis (2), however, is the lack of accretion-type X-rays in Galactic WNL stars in general (Pollock 1987).

Problems with either scenario make it impossible to decide which (if any) is correct. Possibly, the bolometric corrections of WN8,9 stars are smaller than for WN6,7 stars, making the former significantly less luminous and thus less massive. This is favored by Lortet and Testor (1988). I suspect that this problem will only be resolved by some new innovative observational technique.

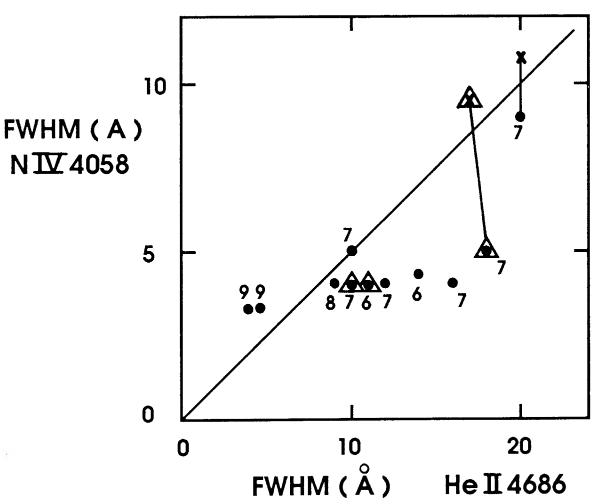

FIG. 10

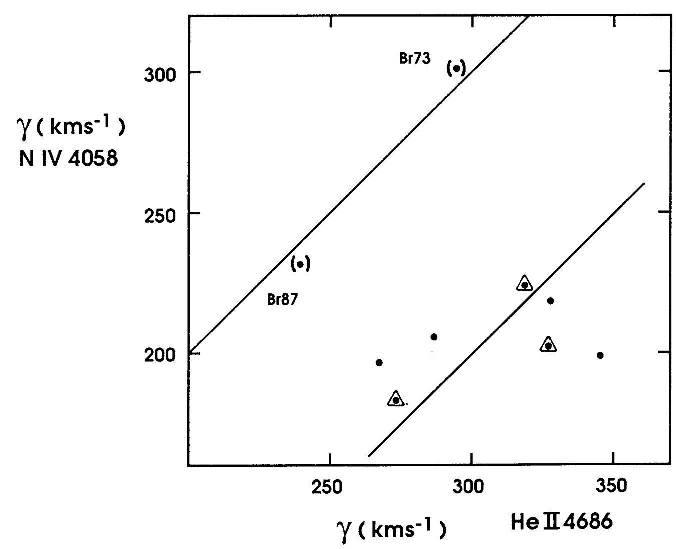

FIG. 11

FIG. 10.—Width of the emission line N IV 4058 vs. width of He II 4686 in the LMC WNL stars observed here. Points refer to photographic spectra, crosses to IDS. Binaries are indicated by triangles. Numbers refer to subclasses. The straight line is a rough fit.

FIG. 11.—Systemic velocity plot of N IV 4058 vs. He II 4686. Triangles indicate binaries. The straight lines have slope unity. Note that Br 73 has inferior quality data, while Br 87 is a multiple W-R system.

TABLE 23

COMPARISON OF WN8,9 AND WN6,7 STARS

Property	WN8,9	WN6,7
Spectrum (optical):		
Emission lines	FWHM ~ 15 Å	FWHM ~ 30 Å
P Cygni	Strong (He I)	None or weak
v_∞	~1500 km s^{-1}	~2500 km s^{-1}
H/He	Very low to moderate	Very low to moderate
Absolute magnitude:		
M_v	-5.6 ± 0.3	-6.1 ± 0.2
B.C.	−4.5:	−4.5
$M_{\rm bol}$	−10.1:	−10.6
Masses:		
Dynamic	No WN8,9 + O binaries	High (~30–60 $M_\odot$)
$M(L)$	High; possibly slightly less than WN6,7	High
Radii[a]:		
$R_{\rm core}$	$\approx 30\ R_\odot$	$\approx 10\ R_\odot$
Variability (nonbinary):		
Continuum, lines, polarization	Strongest of all W-R	Moderate
Binary frequency:		
W-R + O	Low (0 ± 33%)	High (57 ± 19%)
W-R + c	High??	Moderate?
Runaway status:		
Peculiar RV	Often high (e.g., WR 123, WR 124)	A few high
In clusters	No	Yes (e.g. 30 Dor)
Global spatial distribution:		
Galaxy	Found at all R Found ~ everywhere	Found at all R Found ~ everywhere
LMC	$\frac{N(\mathrm{WN8,9})}{N(\mathrm{WN6,7})} \sim 0.3$	

[a] For WN8,9 based on $v_\infty \simeq 3v_{\rm esc}$ (Abott 1982), with $v_{\rm esc} = \sqrt{2GM/R_{\rm core}}$ and $M(\mathrm{WN8,9}) \simeq M(\mathrm{WN6,7})$. For WN6,7 from light curve analysis of CQ Cep (Leung, Moffat, and Seggewiss 1983).

VI. CONCLUSIONS

Despite the difference in metallicity (Z) within the Galaxy and between it on the whole, and the LMC, their WNL populations show no significant differences with regard to masses, luminosities, spatial distribution, number relative to the total W-R population, and proportion of WN8,9 versus WN6,7 stars. This is all the more remarkable in view of the extreme difference in distribution of other W-R subtypes (e.g., most WCL stars occur toward the center of the Galaxy while none are seen in the LMC), which is likely due to differences in Z. This suggests that all massive stars after H-burning evolution are channeled though the WNL phase, regardless of differences in Z. What happens after the WNL phase however, does appear to depend on Z.

The reason for this lack of sensitivity to Z for the WNL stars may be related to the greater similarity of the spectra of WNL stars to their O/Of progenitors than later W-R phases (WNE, WC). Indeed, O and Of stars are found essentially everywhere in the Galaxy and the LMC.

The reason for the stark difference between WN6,7 and WN8,9 stars remains a mystery.

I am grateful for financial assistance from the Natural Sciences and Engineering Research Council of Canada.

REFERENCES

Abbott, D. C. 1982, *Ap. J.*, **259**, 282.
Antokhin, I. I., Aslanov, A. A., and Cherepashchuk, A. M. 1982, *Soviet Astr. Letters*, **8**, 395.
Bracher, K. 1966, Ph.D. thesis, Indiana University.
Breysacher, J. 1981, *Astr. Ap. Suppl.*, **43**, 203.
———. 1986, *Astr. Ap.*, **160**, 185.
Conti, P. S. 1976, *Mém. Soc. Roy. Sci. Liège*, 6e Sér., **9**, 193.
Conti, P. S., Leep, F. M., and Perry, D. N. 1983, *Ap. J.*, **268**, 228.
Conti, P. S., Massey, P., and Garmany, C. D. 1989, *Ap. J.*, submitted.
Conti, P. S., Niemela, V. S., and Walborn, N. R. 1979, *Ap. J.*, **228**, 206.
de Freitas Pacheco, J. A., and Machado, M. A. 1988, *A.J.*, **96**, 365.
Drissen, L., Lamontagne, R., Moffat, A. F. J., Bastien, P., and Séguin, M. 1986*a*, *Ap. J.*, **304**, 188.
Drissen, L., Moffat, A. F. J., Bastien, P., Lamontagne, R., and Tapia, S. 1986*b*, *Ap. J.*, **306**, 215.
Garmany, C. D., and Fitzpatrick, E. L. 1988, *Ap. J.*, **332**, 711.
Gies, D. R., and Bolton, C. T. 1986, *Ap. J. Suppl.*, **61**, 419.
Hidayat, B., Admiranto, A. G., and van der Hucht, K. A. 1984, *Ap. Space Sci.*, **99**, 175.
Isserstedt, J., Moffat, A. F. J., and Niemela, V. S. 1983, *Astr. Ap.*, **126**, 183.
Koenigsberger, G., Firmani, C., and Bisiacchi, G. F. 1980, *Rev. Mexicana Astr. Ap.*, **5**, 45.
Lamontagne, R. 1983, Ph.D. thesis, Université de Montréal.
Lamontagne, R., Moffat, A. F. J., Koenigsberger, G., and Seggewiss, W. 1982, *Ap. J.*, **253**, 230.
Lamontagne, R., Moffat, A. F. J., and Seggewiss, W. 1983, *Ap. J.*, **269**, 596.
Leonard, P. J. T., and Duncan, M. J. 1988, *A.J.*, **96**, 222.
Leung, K.-C., Moffat, A. F. J., and Seggewiss, W. 1983, *Ap. J.*, **265**, 961.
Lortet, M.-C., and Testor, G. 1988, *Astr. Ap.*, **194**, 11.
Lundström, I., and Stenholm, B. 1984, *Astr. Ap. Suppl.*, **58**, 163.
Massey, P. 1981, *Ap. J.*, **244**, 157.
Moffat, A. F. J. 1978, *Astr. Ap.*, **68**, 41.
———. 1981, in *IAU Colloquium 59, Effects of Mass Loss in Stellar Evolution*, ed. C. Chiosi, and R. Stalio (Dordrecht: Reidel), p. 301.
———. 1982, in *IAU Symposium 99, Wolf-Rayet Stars: Observations, Physics, Evolution*, ed. C. W. H. de Loore, and A. J. Willis (Dordrecht: Reidel), p. 515.
———. 1988, *Ap. J.*, **330**, 766.
Moffat, A. F. J., *et al.* 1990, *Ap. J.*, in press.

Moffat, A. F. J., and Isserstedt, J. 1980, *Astr. Ap.*, **91**, 147.
Moffat, A. F. J., Lamontagne, R., and Seggewiss, W. 1982, *Astr. Ap.*, **114**, 135.
Moffat, A. F. J., Lamontagne, R., Shara, M. M., and McAlister, H. A. 1986, *A.J.*, **91**, 1392.
Moffat, A. F. J., and Niemela, V. S. 1982, *Astr. Ap.*, **108**, 326.
———. 1984, *Ap. J.*, **284**, 631.
Moffat, A. F. J., Niemela, V. S., and Marraco, H. 1990, *Ap. J.*, submitted (Paper VI).
Moffat, A. F. J., Niemela, V. S., Phillips, M. M., Chu, Y.-H., and Seggewiss, W. 1987, *Ap. J.*, **312**, 612.
Moffat, A. F. J., and Seggewiss, W. 1978, *Astr. Ap.*, **70**, 69.
———. 1983, *Astr. Ap.*, **125**, 83.
———. 1986, *Ap. J.*, **309**, 714.
Moffat, A. F. J., Seggewiss, W., and Shara, M. M. 1985, *Ap. J.*, **295**, 109 (MSS).
Moffat, A. F. J., and Shara, M. M. 1986, *A.J.*, **92**, 952.
Morgan, S., and Böhm-Vitense, E. 1988, *A.J.*, **96**, 1377.
Niemela, V. S. 1982, in *IAU Symposium 99, Wolf-Rayet Stars, Observations, Physics, Evolution*, ed. C. W. H. de Loore and A. J. Willis (Dordrecht: Reidel), p. 299.
Niemela, V. S., Conti, P. S., and Massey, P. 1980, *Ap. J.*, **241**, 1050.
Pesch, P., Hiltner, W. A., and Brandt, J. C. 1960, *Ap. J.*, **132**, 513.
Pollock, A. M. T. 1987, *Ap. J.*, **320**, 283.
Seggewiss, W., and Moffat, A. F. J. 1979, *Astr. Ap.*, **72**, 332.
Shara, M. M., Potter, M., Moffat, A. F. J., and Smith, L. F. 1989, in *IAU Colloquium 113, Physics of Luminous Blue Variables*, ed. K. Davidson, A. F. J. Moffat, and H. G. L. M. Lamers (Dordrecht: Kluwer), p. 308.
Smith, L. F. 1968, *M.N.R.A.S.*, **138**, 109.
Smith, L. F., and Hummer, D. G. 1988, *M.N.R.A.S.*, **230**, 511.
Smith, A. M., Cornett, R. N., and Hill, R. S. 1987, *Ap. J.*, **320**, 609.
St.-Louis, N., Moffat, A. F. J., Drissen, L., Bastien, P., and Robert, C. 1988, *Ap. J.*, **330**, 286.
Testor, G., Llebaria, A., and Debray, B. 1988, The *ESO Messenger*, No. 54, p. 43.
Torres, A. V. 1988, *Ap. J.*, **325**, 759.
van der Hucht, K. A., Conti, P. S., Lundström, I., and Stenholm, B. 1981, *Space Sci. Rev.*, **28**, 227.
van der Hucht, K. A., Hidayat, B., Admiranto, A. G., Supelli, K. R., and Doom, C. 1988, *Astr. Ap.*, **199**, 217.

A. F. J. Moffat: Département de physique, Université de Montréal, C.P. 6128, Succ. A, Montréal, P.Q., Canada H3C 3J7